PHYSICAL REVIEW A VOLUME 38, NUMBER 10 NOVEMBER 15, 1988

Dynamics of transient domain structures in nematic liquid crystals: The splay Fréedericksz transition

F. Sagués and F. Arias
Departament de Química Física, Universitat de Barcelona, Diagonal 647, Barcelona 08028, Spain
(Received 1 April 1988)

We discuss the dynamics of the transient pattern formation process corresponding to the splay Fréedericksz transition. The emergence and subsequent evolution of the spatial periodicity is here described in terms of the temporal dependence of the wave numbers corresponding to the maxima of the structure factor. Situations of perpendicular as well as oblique field-induced stripes relative to the initial orientation of the director are both examined with explicit indications of the time scales needed for their appearance and posterior development.

I. INTRODUCTION

Many different systems in nature experience nonequilibrium processes characterized by the emergence of spatially periodic order developing spontaneously from a homogeneous state. Liquid crystals constitute an especially well-studied class of such systems. In this paper we will particularly refer to the magnetically induced reorientation of a nematic sample known as a Fréedericksz transition.[1] Very broad theoretical and experimental evidence[2–13] supports the idea that such an orientational transition normally induces hydrodynamic motions that result in the transient appearance of striped textures of characteristic periodicity in the plane of the sample. The earliest observations made by Carr[2] in *N*-(4′-*n*-methoxy)benzylidene-4′ -(*n*-butyl)aniline (MBBA) stimulated the theoretical and experimental analysis of Guyon *et al.*[3] applied to a planar-homeotropic geometry. In this last decade experiments abound both in lyotropics[4–10] and thermotropics[7,8] reporting the occurrence of perpendicular[3,7,9] as well as oblique[8] and two-dimensional[10] striped patterns relative to the initial orientation of the sample. Here we will specifically concentrate on Guyon *et al.*'s geometry,[3] also discussed by Hurd *et al.*,[8] which is especially interesting since oblique periodic structures may result from the coupling of the flow and director fields in three dimensions.

The process under consideration shows strong similarities with other spatial pattern forming phenomena such as those corresponding to the Rayleigh-Bénard or Couette-Taylor instabilities in hydrodynamics, but at the same time it intrinsically differs from these latter ones in its transient nature. Owing to this and following the pioneering analysis by Guyon *et al.*,[3] the field-dependent periodicity of the pattern has been commonly associated[3,7–11] with the wavelength corresponding to the mode of fastest growth predicted by a linear analysis of the nematodynamic equations. This approach, based on an eigenvalue analysis, although useful in understanding the main physical ingredients in the origin of the observed periodic structures, is far less valid if we are interested in the dynamics of the pattern formation process. For this reason we have recently proposed a model[12–14] which identifies the basic time scales involved in the reorientation of the nematic sample. This model enables us to study the time dependence of the characteristic periodicity starting from the homogeneous sample at the initial time. The highlight of our analysis is the evolution equation for the time-dependent structure factor which accounts for the orientational distortions of the director once thermal fluctuations and hydrodynamic effects have been taken into account.

Thermal fluctuations, essential in triggering the initial decay from an unstable state, are incorporated in our description through the use of Langevin-type equations corresponding to a time-dependent Ginzburg-Landau (TDGL) formulation commonly invoked to study critical dynamics[15] and the dynamics of phase transitions.[16] In this way our approach to the problem of the Fréedericksz transition is reminiscent of the Cahn-Hilliard-Cook theory of spinodal decomposition.[17] However, an important conclusion already remarked upon in our previous papers[12,13,18] is that, taking the mean first-passage time (MFPT) as indicator, the equations we use here for the Fréedericksz problem admit linearization procedures that turn out to be valid over a considerably larger time scale than in the case of spinodal decomposition of systems with short-range forces.[19] This should make the predictions contained in this paper much more easily accessible to experimental testing. In the spinodal decomposition problem, it is worth noting that the fact that the most unstable mode is not the homogeneous one can be understood in terms of a conservation law. In the Fréedericksz transition, however, this effect can be related to a tradeoff of rotational for shear viscosities leading to a compromise at some intermediate wave number $\mathbf{q}\neq\mathbf{0}$ for which the increase in elastic energy contribution is favorably balanced by a higher energy dissipation rate controlled by a lower effective viscosity. This effect directly results from the coupling of director rotations and fluid velocity gradients.

Our results here for the dynamics of such a process in the planar-homeotropic geometry indicate that the development of both perpendicular as well as oblique struc-

tures is rather exotic, displaying a rich variety of growth routes. As a matter of fact, since our characterization of the pattern appearance and development proceeds through the analysis of the position in $\mathbf{q}$ space of the maximum of the structure factor, rather peculiar phenomena of competing maxima are found over a wide range of applied magnetic intensities. In addition, situations of emergence of early obliqueness that is finally not persistent and of spurious pattern development are also predicted, as is explained in detail in Sec. IV. Finally, a brief discussion of the effects that the initial prescribed conditions and the material parameters have on the pattern development is also presented.

The paper is organized as follows. In Sec. II we review the general dynamical equations satisfied by the director components. Section III is essentially devoted to deriving the corresponding equations for the components of the structure factor. The main results and their discussion are summarized is Sec. IV, whereas Sec. V is reserved for raising some conclusions and suggesting future perspectives. Finally, the more technical points are reserved for the Appendixes.

II. EQUATIONS FOR THE PLANAR-HOMEOTROPIC FRÉEDERICKSZ TRANSITION

Let us assume a parallel-plate cell of thickness d containing planar-aligned nematic liquid crystals with $\chi_a > 0$. The initial director characterizing the internal orientation of the slab is arbitrarily prescribed along the x direction: $\mathbf{n}^0=(1,0,0)$. Then at some initial time the molecules of the sample are suddenly forced to rotate towards the normal to the walls by applying an external magnetic field along the z direction, $\mathbf{H}=(0,0,H)$, with intensity H exceeding a critical threshold for distortion. As we mentioned in the Introduction Hurd *et al.*[8] reported on the emergence of a transient periodic structure that for certain values of H appears under cross polarizers as oblique stripes in the x-y plane. Flows characteristic of convection cells develop in some plane across the stripes. This obliges us to simultaneously refer to the coupled dynamics of both the director and velocity fields. For the director we will restrict our discussion to the components n_y and n_z which become macroscopically amplified during the realignment. Using a minimal-coupling approximation,[20] the nematodynamic equations written in terms of functional derivatives of the free energy $\mathcal{F}\{\mathbf{n}(\mathbf{r};t);\mathbf{v}(\mathbf{r};t)\}$ (Ref. 21) read (summation over repeated indices generically denoted α is implied) as shown in Eq. (2.1). Equations (2.1) are obtained by specializing for the geometry considered here the model equations we derived in Ref. 12, where a complete discussion of the principles used in their formulation may also be found. In Appendix A and for the sake of the self-completeness of the paper we provide the reader with an extracted and directly utilizable version of those general equations. In (2.1) ρ is the mass density, γ_1, γ_2 ($\lambda=-\gamma_2/\gamma_1$), ν_1, ν_2, and ν_3 are the viscosity coefficients used in Harvard's version of the nematodynamic equations, and p is the pressure. The Gaussian random forces left in (2.1) represent sources of thermal noise and accordingly they are prescribed with

$$
d_{t'}\begin{Bmatrix} n_y \\ n_z \\ v_x \\ v_y \\ v_z \end{Bmatrix} =
\begin{pmatrix}
-\frac{1}{\gamma_1} & 0 & \frac{1}{2\rho}(\lambda-1)\partial_y & 0 & 0 \\
0 & -\frac{1}{\gamma_1} & \frac{1}{2\rho}(\lambda-1)\partial_z & 0 & 0 \\
\frac{1}{2\rho}(\lambda-1)\partial_y & \frac{1}{2\rho}(\lambda-1)\partial_z & \frac{1}{\rho^2}[2\nu_1\partial_x^2+\nu_3(\partial_y^2+\partial_z^2)] & \frac{1}{\rho^2}\nu_3\partial_{xy}^2 & \frac{1}{\rho^2}\nu_3\partial_{xz}^2 \\
\frac{1}{2\rho}(\lambda+1)\partial_x & 0 & \frac{1}{\rho^2}\nu_3\partial_{xy}^2 & \frac{1}{\rho^2}[\nu_3\partial_x^2+\nu_2(2\partial_y^2+\partial_z^2)] & \frac{1}{\rho^2}\nu_2\partial_{yz}^2 \\
0 & \frac{1}{2\rho}(\lambda+1)\partial_x & \frac{1}{\rho^2}\nu_3\partial_{xz}^2 & \frac{1}{\rho^2}\nu_2\partial_{yz}^2 & \frac{1}{\rho^2}[\nu_3\partial_x^2+\nu_2(\partial_y^2+2\partial_z^2)]
\end{pmatrix}
\begin{Bmatrix} \frac{\delta\mathcal{F}}{\delta n_y} \\ \frac{\delta\mathcal{F}}{\delta n_z} \\ \frac{\delta\mathcal{F}}{\delta v_x} \\ \frac{\delta\mathcal{F}}{\delta v_y} \\ \frac{\delta\mathcal{F}}{\delta v_z} \end{Bmatrix}
+
\begin{Bmatrix} 0 \\ 0 \\ -\frac{1}{\rho}\partial_x p \\ -\frac{1}{\rho}\partial_y p \\ -\frac{1}{\rho}\partial_z p \end{Bmatrix}
+
\begin{Bmatrix} \xi_y \\ \xi_z \\ \partial_\alpha \xi_{\alpha x} \\ \partial_\alpha \xi_{\alpha y} \\ \partial_\alpha \xi_{\alpha z} \end{Bmatrix}, \quad \alpha=(x,y,z) . \tag{2.1}
$$

zero mean value and satisfying the appropriate fluctuation-dissipation relations (see Appendix A)

$$\langle \xi_\alpha(\mathbf{r}_1,t_1')\xi_\beta(\mathbf{r}_2,t_2')\rangle = 2\delta_{\alpha\beta}\frac{k_B T}{\gamma_1}\delta(\mathbf{r}_1-\mathbf{r}_2)\delta(t_1'-t_2') ,$$
$$\langle \xi_{\alpha\beta}(\mathbf{r}_1,t_1')\xi_{\delta\gamma}(\mathbf{r}_2,t_2')\rangle = 2k_B T M^0_{\alpha\beta\delta\gamma}\delta(\mathbf{r}_1-\mathbf{r}_2)\delta(t_1'-t_2') , \quad (2.2)$$

where $M^0_{\alpha\beta\delta\gamma}$ stands for the tensor $M_{\alpha\beta\delta\gamma}$ introduced in (A6) written in terms of $\mathbf{n}^0$. Finally, the explicit expressions for the functional derivatives of the free energy are computed in the limit of small distortions leading to

$$\frac{\delta\mathcal{F}}{\delta n_y} = -K_1(\partial_y^2 n_y+\partial_{yz}^2 n_z)-K_2(\partial_z^2 n_y-\partial_{yz}^2 n_z) - K_3\partial_x^2 n_y ,$$
$$\frac{\delta\mathcal{F}}{\delta n_z} = -K_1(\partial_{yz}^2 n_y+\partial_z^2 n_z)-K_2(\partial_y^2 n_z-\partial_{yz}^2 n_y) - K_3\partial_x^2 n_z-\chi_a H^2 n_z , \quad (2.3)$$
$$\frac{\delta\mathcal{F}}{\delta v_\alpha} = \rho v_\alpha, \quad \alpha=\{x,y,z\} .$$

As we anticipated in the Introduction, we intend to follow the dynamics of the Fréedericksz instability by focusing on the temporal evolution of the orientational distortions n_y and n_z. Thus our primary goal consists now in reducing (2.1) to a pair of closed equations for these two components of the director. This is accomplished by successive technical manipulations of (2.1). Here we limit ourselves to carefully describing the different steps of this standard procedure that can be in this way straightforwardly reproduced by the interested reader.

(i) We make the common approximation of negligible inertia.[3,7–9,12–14] In addition, pressure terms can be easily eliminated from the velocity equations in two steps using the fact that $\nabla\cdot(\nabla p)=0$. First we take partial derivatives relative to y and x, respectively, in the equations for v_x and v_y and after that we repeat exactly the same procedure but now for the pair v_x, v_z. Finally, by invoking the incompressibility condition of the nematic materials we are able to get rid of one of the velocity components.

(ii) We introduce a Fourier representation corresponding to the free-free boundary conditions we adopt throughout the paper: $\partial_z v_x=\partial_z v_y=v_z=n_z=0$ at $z=\pm d/2$. Specifically, we set

$$\begin{bmatrix} v_\alpha \\ n_\alpha \\ \xi_\alpha \\ \zeta_{\alpha\beta}\end{bmatrix}(\mathbf{r};t') = \sum_{\mathbf{q},k_z}\begin{bmatrix} v_\alpha \\ n_\alpha \\ \xi_\alpha \\ \zeta_{\alpha\beta}\end{bmatrix}_{\mathbf{q},k_z}(t')e^{i\mathbf{q}\cdot\rho}\sin(k_z z) ,$$
$$\begin{bmatrix} v_z \\ n_z \\ \xi_z \\ \zeta_{xz} \\ \zeta_{yz}\end{bmatrix}(\mathbf{r};t') = \sum_{\mathbf{q},k_z}\begin{bmatrix} v_z \\ n_z \\ \xi_z \\ \zeta_{xz} \\ \zeta_{yz}\end{bmatrix}_{\mathbf{q},k_z}(t')e^{i\mathbf{q}\cdot\rho}\cos(k_z z) , \quad (2.4)$$

for $\alpha,\beta\neq z$ (except for ζ_{zz}), with $k_z=(2m+1)\pi/d$. A detailed discussion regarding the appropriateness of the free-free boundary conditions adopted here may be found in the paper by Hurd *et al.*[8]

(iii) We specialize our analysis to the most unstable z mode associated to an even z symmetry for n_z. It corresponds to $m=0$ or $k_z=\pi/d$. This enables us to use for the remainder of the paper dimensionless wave numbers $\mathbf{Q}=\mathbf{q}/(\pi/d)$. Complementarily we propose a time adimensionalization, $t'=\tau_0 t$, based on the time unit corresponding to pure orientational relaxations: $\tau_0=\gamma_1/(K_1\pi^2/d^2)=\gamma_1/(\chi_a H_c^2)$, H_c being the critical magnetic intensity for the pure splay Fréedericksz transition.

When all these transformations have been completed we end up with a pair of coupled equations for the Fourier amplitudes $(n_{y;\mathbf{Q}}(t);n_{z;\mathbf{Q}}(t))$ which are more compactly written using a matrix notation:

$$\underline{\gamma}\,\partial_t\bar{n}=\underline{K}\bar{n}+\bar{\psi}, \quad \bar{n}\equiv\bar{n}_{\mathbf{Q}}(t)=\begin{bmatrix} n_{y;\mathbf{Q}}(t) \\ n_{z;\mathbf{Q}}(t)\end{bmatrix} \quad (2.5)$$

$\underline{\gamma}$ and $\underline{K}$ are self-adjoint matrices, respectively, associated with the viscosity and elastic contributions, whereas $\bar{\psi}$ collects the entire effect of thermal fluctuations. The explicit expressions for the $\underline{\gamma}$, $\underline{K}$, and $\bar{\psi}$ components in terms of the viscosity and elastic constants of the material are given in Appendix B. Operating (2.5) with $\underline{\gamma}^{-1}$ we transform this last equation into the more convenient form

$$\partial_t\bar{n}=\underline{\Lambda}\bar{n}+\bar{\eta} ,$$
$$\langle \eta_{\alpha;\mathbf{Q}}(t_1)\eta_{\beta;-\mathbf{Q}}(t_2)\rangle = 2\epsilon_{\alpha\beta;\mathbf{Q}}\delta(t_1-t_2) , \quad (2.6)$$

with $\underline{\gamma}^{-1}\underline{K}=\underline{\Lambda}$ and $\underline{\gamma}^{-1}\bar{\psi}=\bar{\eta}$.

As a way of testing (2.6), let us carefully examine the particular case of the planar Fréedericksz transition with perpendicular stripes which can be easily discussed in terms of Eq. (2.6). In particular, we will concentrate on the structure of the matrix $\underline{\Lambda}$ responsible for the deterministic part of the dynamics of the director.

The case of perpendicular stripes: $Q_x\neq 0$, $Q_y=0$

This is the situation considered by Guyon *et al.*[3] in their experimental observations on thick samples of MBBA. In our analysis here we have only to project the obtained equations onto the subspace $Q_y=0$. The $\underline{\Lambda}$ adopts a diagonal form with the pair of eigenvalues λ_y,λ_z corresponding, respectively, to n_y, n_z, given by

$$\lambda_y = -\frac{1}{1-\frac{1}{\gamma_1}\frac{\alpha_2^2}{\eta_c+\eta_a Q_x^{-2}}}(\bar{K}_2+\bar{K}_3 Q_x^2) ,$$
$$\lambda_z = \frac{1}{1-\frac{1}{\gamma_1}\frac{(\alpha_3-\alpha_2 Q_x^2)^2}{\eta_c Q_x^4+2(\nu_1-\eta_4+\eta_a)Q_x^2+\eta_b}} \times(h^2-1-\bar{K}_3 Q_x^2) . \quad (2.7)$$

In (2.7), $\eta_a,\eta_b,\eta_c,\alpha_2,\alpha_3,\eta_4$ are viscosity coefficients defined in Appendix B, $\bar{K}_2,\bar{K}_3$ are reduced elastic constants, $\bar{K}_i=K_i/K_1$, and h^2 is the reduced magnetic inten-

sity, $h^2=H^2/H_c^2$. When $Q_y=0$ there is no coupling between the perpendicular components n_y and n_z. Consequently, and according to the physical image of the Fréedericksz transition, we may predict that the unique component of the director susceptible of experiencing the instability will be n_z, while n_y will remain in any case stable. Indeed, based on values in the literature for MBBA,[1]

$$1-(\alpha_2^2/\gamma_1\eta_c)/(1+\eta_a/\eta_c Q_x^{-2})$$

is positive and consequently λ_y is always negative. On the other hand, the expression for λ_z coincides exactly with the one computed in Ref. 3, if we realize that in that paper a different notation for the viscosity parameters was used ($\eta_b\to\eta_1$, $\eta_c\to\eta_2$), and additionally it was assumed $K_1=K_3$. Moreover, the particularly simple expression for λ_z when $Q_y=0$ is especially appropriate in order to better understand the origin of inhomogeneous patterns, $Q_x\neq 0$, leading the response of the system to the instability: the additional contributions corresponding to internal bend distortions, $-\bar{K}_3 Q_x^2$, are favorably balanced by a lower value of the effective viscosity,

$$\gamma_1^*/\gamma_1=1-\frac{1}{\gamma_1}(\alpha_3-\alpha_2 Q_x^2)^2/[\eta_c Q_x^4+2(\nu_1-\eta_4+\eta_a)Q_x^2+\eta_b]\ ,$$

which monotonously decreases from a maximum value, $1-\alpha_3^2/\gamma_1\eta_b$, at $Q_x=0$ to a minimum, $1-\alpha_2^2/\gamma_1\eta_c$ for $Q_x\to\infty$.

The complementary situation, $Q_x=0$, $Q_y\neq 0$, which would correspond to a striped texture parallel to the initial orientation, has been neither reported in the literature, nor predicted in our analysis here (see Sec. IV).

III. THE DYNAMICS OF THE STRUCTURE FACTOR

In a general situation of nonzero wave number Q_y the algebra is more complicated since the equations for n_y and n_z are nontrivially coupled. To proceed further we need to diagonalize $\bar{\Lambda}$:

$$(\underline{U}\underline{\Lambda}\,\underline{U}^{-1})_{\alpha\beta}=\lambda_\alpha\delta_{\alpha\beta}\ . \tag{3.1}$$

By defining

$$\bar{m}=\underline{U}\bar{n},\quad \bar{\varphi}=\underline{U}\bar{\eta}\ , \tag{3.2}$$

Eq. (2.6) transforms into

$$\dot{m}_\alpha=\lambda_\alpha m_\alpha+\varphi_\alpha,\quad \alpha=\{y,z\}\ . \tag{3.3}$$

These Langevin-type equations can be directly converted into evolution equations for the components of structure factor $\langle m_{\alpha;\mathbf{Q}}(t)m_{\beta;-\mathbf{Q}}(t)\rangle$. In terms of the intensity of the thermal noise sources

$$\begin{aligned}\langle\varphi_{\alpha;\mathbf{Q}}(t_1)\varphi_{\beta;-\mathbf{Q}}(t_2)\rangle&=2\Phi_{\alpha\beta;\mathbf{Q}}\delta(t_1-t_2)\\&=2U_{\alpha\alpha'}U_{\beta\beta'}\epsilon_{\alpha'\beta';\mathbf{Q}}\delta(t_1-t_2)\end{aligned} \tag{3.4}$$

we have

$$\langle m_{\alpha;\mathbf{Q}}(t)m_{\beta;-\mathbf{Q}}(t)\rangle=\exp[(\lambda_\alpha+\lambda_\beta)t]\langle m_{\alpha;\mathbf{Q}}(0)m_{\beta;-\mathbf{Q}}(0)\rangle+2\frac{\Phi_{\alpha\beta;\bar{Q}}}{\lambda_\alpha+\lambda_\beta}\{\exp[(\lambda_\alpha+\lambda_\beta)t]-1\}\ . \tag{3.5}$$

The physical components of the structure factor are then finally given by

$$\begin{aligned}S_{\alpha\beta}(\mathbf{Q};t)&\equiv\langle n_{\alpha;\mathbf{Q}}(t)n_{\beta;\mathbf{Q}}(t)\rangle\\&=U_{\alpha\rho}^{-1}U_{\rho\rho'}U_{\beta\gamma}^{-1}U_{\gamma\gamma'}\exp[(\lambda_\rho+\lambda_\gamma)t]\\&\quad\times\left[S_{\rho'\gamma'}(\mathbf{Q},0)+2\frac{\epsilon_{\rho'\gamma'}}{\lambda_\rho+\lambda_\gamma}\{1-\exp[-(\lambda_\rho+\lambda_\gamma)t]\}\right]\end{aligned} \tag{3.6}$$

expressed in terms of the initial correlations between the director components $S_{\rho'\gamma'}(\mathbf{Q},0)$. These initial conditions are consistently obtained taking the long-time limit on the solution (3.6) for magnetic intensities below the critical one: $h_i^2<1$.

The emergence and growth of the periodic structures resulting from the Fréedericksz transition is followed by studying the time-dependent structure factor $S_{\alpha\beta}(\mathbf{Q};t)$. The position in $\mathbf{Q}$ space of the maximum of $S_{\alpha\beta}(\mathbf{Q};t)$, denoted $\mathbf{Q}_{\max}(t)$, is associated with the characteristic wave number of the striped texture and its temporal evolution from $\mathbf{Q}=\mathbf{0}$ with the pattern development.

The role of thermal fluctuations incorporated consistently from the beginning into the model considered here is essential in describing the dynamics of the unstable distortion modes, as can be seen in the final results (3.6). Fluctuation effects appear there through two well-differentiated contributions: thermal randomness in the initial conditions corresponding to the first term in (3.6) and subsequent spreading of stochastic trajectories represented by the additive correction $\epsilon_{\rho'\gamma'}$. At $t=0$ initial conditions dominate and we can expect that the homogeneous mode $\mathbf{Q}=\mathbf{0}$ will be preponderant. In the other limit, $t\to\infty$, the evolution of $S(\mathbf{Q};t)$ is largely

dominated by the exponential factors. In this way the growth of the structure factor will be eventually dominated by the mode of the fastest growth, this is by the Q maximum of the unstable eigenvalue λ_z.[22] Consequently our results for $Q_{max}(t)$ will asymptotically approach as time goes on those predicted in the eigenvalue analysis of Hurd *et al.*[8] The merit of (3.6) is that it enables us to describe the whole temporal evolution of $Q_{max}(t)$ between these two limits. This is the purpose of Sec. IV.

IV. DYNAMICS OF PATTERN GROWTH

The results in this section refer to the z-diagonal component of the structure function, $S_{zz}(\mathbf{Q},t)$. In other words, we will limit ourselves to studying the pattern of evolution of the orientational distortions along the direction of the applied magnetic field. As a matter of fact, $S_{yy}(\mathbf{Q},t)$ essentially displays analogous trends of behavior with some specificities, limited to very short time intervals after the initial destabilization of the sample, probably originating in initial condition effects. The most interesting questions we want to emphasize regarding the phenomenon of the transient pattern development examined here will be presented in relation with particular examples of application of Eq. (3.6) for $S_{zz}(\mathbf{Q},t)$.

Let us start, for example, with the dynamics we have reproduced in Figs. 1 and 2, corresponding to an applied reduced magnetic intensity $h^2=10$ and initial conditions for $h_i^2=0.5$. Figure 1 is a direct three-dimensional representation of $S_{zz}(\mathbf{Q},t)$ versus (Q_x^2,Q_y^2) at different times, whereas Fig. 2 is somewhat more illustrative of the pattern growth route since it monitors the dynamics of $Q_{max}(t)$. The interesting aspect to be noticed in Fig. 2 is the permanent maximum exhibited by S_{zz} at the origin of wave numbers $\mathbf{Q}=\mathbf{0}$. According to what is depicted we can distinguish several phases in the emergence and development of the spatial pattern. In an initial stage, the homogeneous mode $\mathbf{Q}=\mathbf{0}$ dominates as is expected and no other maximum exists. The distribution of orientational distortions is still reminiscent of the Ornstein-Zernike form corresponding to the equilibrium fluctuations at $h_i^2=0.5<1$. Then, at a very characteristic time, $t\simeq 0.25$ in the units of τ_0,[23] another maximum appears, this one associated with an oblique $\mathbf{Q}\neq\mathbf{0}$ mode. The preponderancy of the trivial maximum at the homogeneous mode $\mathbf{Q}=\mathbf{0}$ lasts for a very short time since a bit later ($t\simeq 0.40$) it is finally dominated by the incipient $\mathbf{Q}\neq\mathbf{0}$ maximum. At this moment the final stage of the evolution is initiated and follows an asymptotic path of slow growth of Q_{max} tending to the value predicted in a deterministic analysis. However, we tend to think that what we have reported here is not, properly speaking, a signature of strict bimodality, since one of the maxima is always associated with the homogeneous mode. The persistence of various maxima of the structure function, even in the asymptotic limit $t\rightarrow\infty$ as is illustrated by this example, is certainly a peculiar feature of the planar-homeotropic Fréedericksz transition we did not find in other simpler geometries analyzed previously,[12,13] as for example for the pure twist distortion.[24] Note also that this result leads us to think of a possible discontinuity in the pattern formation phenomenon contrary to the view of this process as a continuous evolution from the initial preponderant homogeneous mode $\mathbf{Q}=\mathbf{0}$ towards the asymptotic value of maximum growth. Needless to say, this genuine property can only be properly detected and examined in the context of a dynamical treatment such as the one proposed here but is out of the scope of any previous deterministic approach based on eigenvalue determination and analysis.

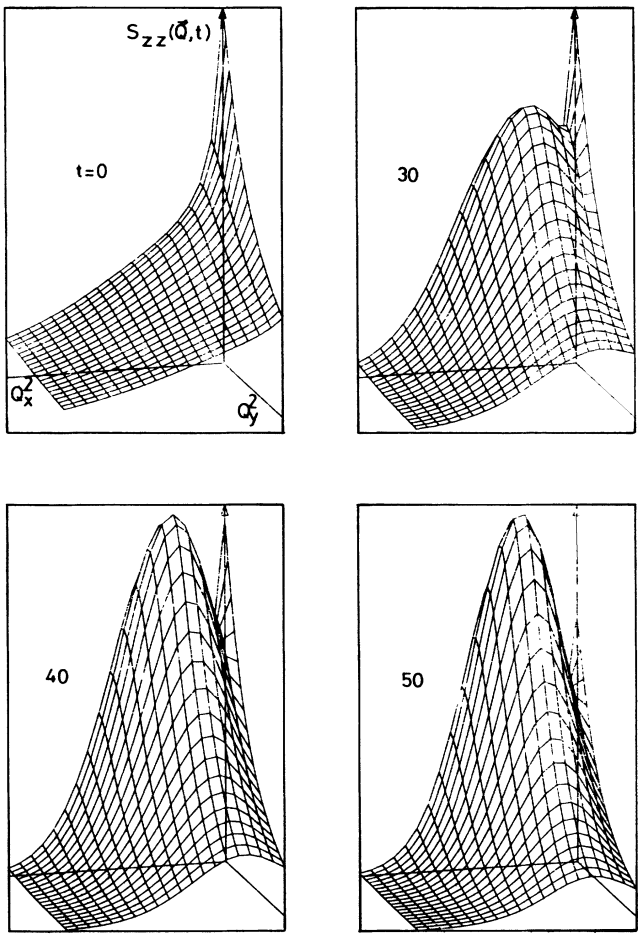

FIG. 1. Different plots for the z-diagonal component of the structure factor vs Q_x^2 and Q_y^2 corresponding to successive stages of the evolution of the orientational fluctuations when the reduced magnetic field is increased from $h_i^2=0.5$ to 10. Times are taken at $t=0$, 30, 40, and 50 measured in units of $\tau_0\simeq 10$ sec in this figure and the subsequent ones. The values for the material parameters are $\eta_a=41.6$ cP, $\eta_b=23.8$ cP, $\eta_c=103.5$ cP, $\nu_1=50.8$ cP, $\gamma_1=76.3$ cP, $\bar{K}_2=\frac{3}{5}$, $\bar{K}_3=\frac{8}{5}$.

Now we turn to the question of the pattern obliqueness. After completing a series of runs for different values of the pair of applied magnetic intensities, (h^2,h_i^2), we conclude that the values of h^2 for which asymptotic oblique patterns may be predicted are independent of h_i^2 and, for the set of material parameters corresponding to MBBA at room temperatures,[1] range from $h^2=5.85$ up to 25.97. For $h^2<5.85$ no asymptotic pattern is predicted and for $h^2>25.97$ they asymptotically adopt perpen-

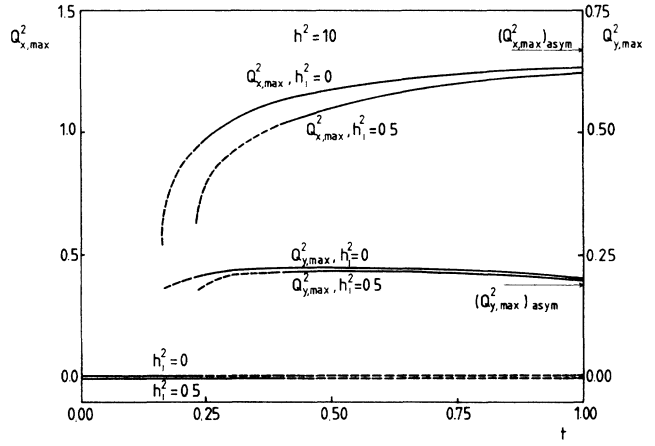

FIG. 2. Wave numbers corresponding to the maxima of the z-diagonal component of the structure factor vs time for an applied reduced magnetic intensity $h^2=10$ and two different initial conditions, $h_i^2=0$ and 0.5. Scales for the x and y components of Q^2_{max} are depicted in the left and right margins, respectively. The dashed lines indicate that the associated maximum is not the dominant one. The asymptotic values obtained in an eigenvalue analysis $[(Q^2_{x,max})_{asym}=1.34,\ (Q^2_{y,max})_{asym}=0.19]$ are also shown for comparison.

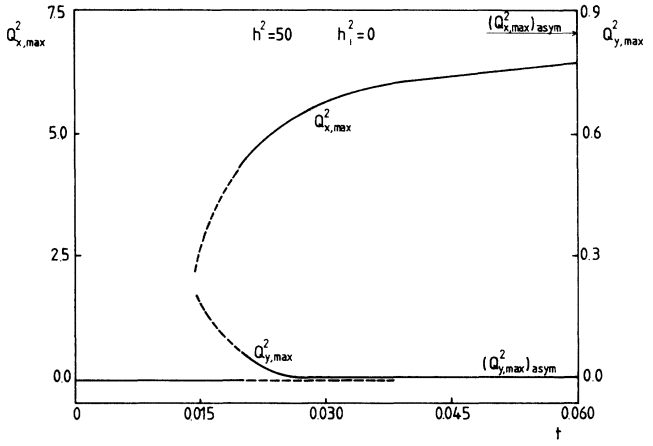

FIG. 3. Evolution of the maxima of $S_{zz}(\mathbf{Q};t)$ vs time for $h^2=50$ and $h_i^2=0$. The maximum corresponding to the homogeneous mode $\mathbf{Q}=\mathbf{0}$ disappears at $t\simeq 0.037$.

dicular orientations relative to the initial alignment of the director. These conclusions essentially agree with what was found in Ref. 8. From a dynamical point of view what remains to be investigated is the interesting dynamics of the obliqueness itself. In other words, we want to elucidate two complementary questions concerning, respectively, the possibility of a pattern development for $5.85<h^2<25.97$ first appearing as perpendicular, $Q_{y,max}=0$, and turning progressively towards an oblique conformation, $(Q_{y,max})_{asym}\neq 0$, and the opposite situation for $h^2>25.97$ in which, although the oblique character of the pattern is not persistent, it may actually appear as a transient. In respect to the first question we have not found any example appropriate to that behavior. Indeed, in all the runs we have performed with $5.85<h^2<25.97$ the dominant inhomogeneous mode naturally changes with time but it is oblique from the very beginning. However, we have been more lucky in regard to the second question since we have effectively found cases for $h^2>25.97$ in which the obliqueness of the pattern may be transitorily detected. This is shown in Fig. 3 where we have plotted the dynamics of $\mathbf{Q}_{max}(t)$ for a considerably larger magnetic field, $h^2=50$ and $h_i^2=0$. Another circumstance deserves our attention in this case and refers to the coexistence of maxima. Although it manifests itself again in this situation, it is not persistent contrary to what was found for $h^2=10$. Comparing both situations we tend to believe that this feature would be practically unobservable in going to larger values of the magnetic forcing.

Finally, we turn to the last point we will explicitly consider here. It is summarized in Fig. 4, corresponding to an applied reduced magnetic intensity $h^2=5.5$, $h_i^2=0$. As we have just mentioned we cannot expect to find in this case a nonhomogeneous mode leading the asymptotic evolution of the structure function. This is exactly what is observed but coexisting with the maximum corresponding to the homogeneous mode $\mathbf{Q}=\mathbf{0}$ another one for $\mathbf{Q}\neq\mathbf{0}$ develops after a transient and even survives a long-time limit. In referring to the z-diagonal component of the structure factor, as we are doing here, we can somewhat qualify this $\mathbf{Q}_{max}\neq\mathbf{0}$ as spurious since it never dominates the maximum at $\mathbf{Q}=\mathbf{0}$, but in examining this particular aspect for the transverse y-diagonal component, $S_{yy}(\mathbf{Q},t)$, we have actually found a few examples of transitory preponderancy of such an inhomogeneous mode.

The final discussion of our results refers to the effects caused by varying the initial conditions of the nematic layer and its material parameters, especially its viscous and elastic constants. In respect to the influence of the

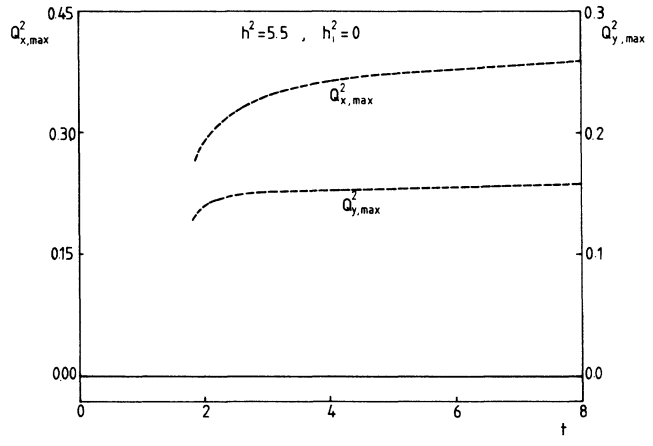

FIG. 4. Evolution of the maxima of $S_{zz}(\mathbf{Q},t)$ vs time corresponding to a reduced magnetic field $h^2=5.5$, $h_i^2=0$. The inhomogeneous mode ($\mathbf{Q}_{max}\neq\mathbf{0}$) never dominates the maximum at $\mathbf{Q}=\mathbf{0}$.

initial magnetic field h_i^2 we have observed that the growth of the pattern is faster when decreasing h_i^2 in complete agreement with what was reported in Ref. 12 for a pure twist Fréedericksz distortion. This is shown in Fig. 2 where as a supplement to the previously considered situation $h^2=10$, $h_i^2=0.5$ we have plotted the results corresponding to $h^2=10$ but with different initial conditions corresponding to $h_i^2=0$. In what concerns the influence of the viscosity and elasticity parameters we have examined separately their effect on Q_x and Q_y. Starting with the wave number Q_x reproducing the periodicity along the initial direction of alignment, it is clear that this periodicity is basically dictated in the bulk of the sample by bend modes, while splay contributions can only play a limited role in narrow boundary layers stretching all along the containing plates. Due to that we can predict that the most important effects have to be observed in relation to variations of K_3, the bend elastic constant. This is what is effectively reproduced in Fig. 5(a), which corresponds to a magnetic forcing from $h_i^2=0.5$ up to 20. For the sake of completeness we have also included additional results corresponding to changes in the specific viscosities which turn out to be more determinant of the pattern growth, i.e., η_b, the Miesowicz shear viscosity for elongated molecules sliding longitudinally, and ν_1 which applied to pure elongational flow. Now, turning our attention to Q_y, the wave-number component directly responsible for the obliqueness of the pattern, it is easily seen that it is directly associated with twist distortions. As a consequence the value of K_2, the twist elastic constant, is of crucial importance in determining the degree of obliqueness of the transitory pattern. Actually, we can practically suppress this obliqueness even from quite the very beginning of the transition after a moderate increase of K_2 as is depicted in Fig. 5(b). Among the viscosities, η_b and ν_1 are again the most significative constants. In particular, the fact that a larger value of ν_1 favors the obliqueness of the periodic texture may be interpreted in the sense that the dissipation for the elongational flow along the x direction, $\nu_1 v_{x,x}^2$, can be considerably reduced due to the incompressibility of the medium if we allow for components of transverse flows in the perpendicular y direction.[25]

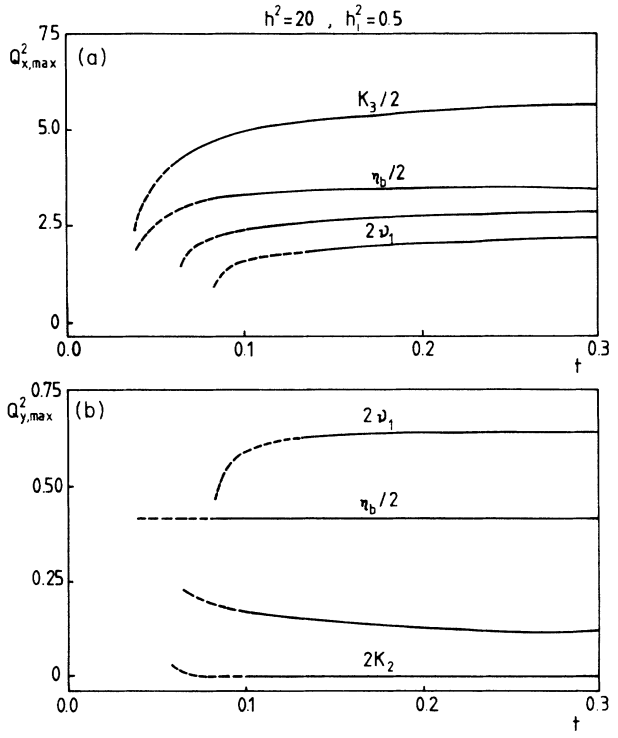

FIG. 5. Evolution of the maxima of $S_{zz}(\mathbf{Q};t)$ vs time for different values of the material parameters. In all the cases $h^2=20$ and $h_i^2=0.5$. (a) shows the influence of K_3, η_b, and ν_1 in the x component of $\mathbf{Q}_{max}$ and (b) shows the influence of K_2, η_b, and ν_1 in the y component.

V. CONCLUSIONS AND OUTLOOK

Motivated by our interest in studying phenomena of spatial symmetry breaking and pattern formation in nonequilibrium physical systems we have directed our attention to the problem of the appearance of transitory periodic structures resulting from the Fréedericksz instability in nematic liquid crystals. We have examined here the planar-homeotropic transition that offers the possibility of predicting the existence of oblique patterns for a wide range of applied magnetic intensities. By using a dynamical model which reproduces the pattern development by means of the temporal evolution of the structure factor we have been able to discuss a large variety of growth routes. Among others we have mainly referred to situations of competing maxima that might well trigger abundant speculations about the continuity or discontinuity of the pattern forming process. In addition, the possibility of finding "spurious patterns," according to the terminology adopted in Sec. IV, has been mentioned and illustrated with a particular example.

The large diversity of pattern growth mechanisms accompanying the pure Fréedericksz reorientation confirms the usefulness of the dynamic treatment adopted here with respect to the previous approaches existent in the literature based on eigenvalue analysis. In addition, our hope is that our work can provoke a renewed experimental interest in the detailed mechanisms of this pattern development.

ACKNOWLEDGMENTS

Thanks are due to X. Giménez for helping us prepare Fig. 1. Partial financial support from Comisión Asesora de Investigación Científica y Técnica (CAICYT) Project No. PR-84-0361 is acknowledged.

APPENDIX A

In this appendix we limit ourselves to recalling what is essential of the general model derived in Ref. 12. For a vectorial field

$$\bar{\phi}(\mathbf{r};t)=(\mathbf{n}(\mathbf{r},t),\mathbf{v}(\mathbf{r},t),\mathbf{u}(\mathbf{r},t))$$

including director, velocity, and position fields we write the following Langevin-type equations:

$$d_t\phi_i = A_{ij}(\bar{\phi})\frac{\delta\mathcal{F}}{\delta\phi_j} + f_i, \quad i=1,\ldots,9$$
$$\bar{f} = (\xi, \partial_\alpha \zeta_{\alpha\beta}, \mathbf{0}) , \tag{A1}$$

in terms of a free-energy $\mathcal{F}$ built up from contributions arising in distortions, translational energy of the molecules, and hydrodynamic pressure. The operator $\underline{A}$ has a dissipative (self-adjoint) contribution $\underline{A}^0$ and a nondissipative (antiadjoint) part $\underline{A}^R$

$$A^0_{ij} = \begin{bmatrix} -\frac{1}{\gamma_1} I & 0 & 0 \\ 0 & L & 0 \\ 0 & 0 & 0 \end{bmatrix}, \quad (A^0_{ij})^\dagger = A^0_{ij} \tag{A2}$$

$$A^R_{ij} = \begin{bmatrix} 0 & \Gamma & 0 \\ -\Gamma^\dagger & 0 & -\frac{1}{\rho} I \\ 0 & \frac{1}{\rho} I & 0 \end{bmatrix}, \quad (A^R_{ij})^\dagger = -A^R_{ij} \tag{A3}$$

where we have used a block notation in which each matrix element represents a 3×3 matrix and I is the identity matrix. The adjoint operator is to be understood here in the sense of integration by parts and transposing matrix indices. The noise sources f_i satisfy a set of general fluctuation-dissipation relations with the dissipative part of the tensor A

$$\langle f_i(\mathbf{r}_1,t_1') f_j(\mathbf{r}_2,t_2')\rangle = -2k_B T A^0_{ij}\delta(\mathbf{r}_1-\mathbf{r}_2)\delta(t_1'-t_2') . \tag{A4}$$

The tensor Γ and L in (A2) and (A3) are given by

$$\Gamma_{\beta\gamma}(\mathbf{n}) = \frac{1}{2\rho}[(\lambda+1)n_\alpha\partial_\alpha\delta_{\beta\gamma} + (\lambda-1)n_\alpha\partial_\beta\delta_{\alpha\gamma}] , \tag{A5}$$

$$L_{\beta\gamma}(\mathbf{n}) = \partial_\alpha M_{\alpha\beta\delta\gamma}(\mathbf{n})\partial_\delta , \tag{A6}$$

$$M_{\alpha\beta\delta\gamma}(\mathbf{n}) = \frac{1}{\rho^2}[2(\nu_1+\nu_2-2\nu_3)n_\alpha n_\beta n_\delta n_\gamma + \nu_2(\delta_{\beta\gamma}\delta_{\alpha\delta}+\delta_{\alpha\gamma}\delta_{\beta\delta} + (\nu_3-\nu_2)(n_\alpha n_\delta\delta_{\gamma\beta}+n_\alpha n_\gamma\delta_{\delta\beta}+n_\beta n_\delta\delta_{\gamma\alpha}+n_\beta n_\gamma\delta_{\delta\alpha})] . \tag{A7}$$

APPENDIX B

To compare with the results of Ref. 8 we adopt here as primary viscosity coefficients the following set: rotational viscosity, γ_1; viscosity for elongational flow, ν_1; and the Miesowicz shear viscosities η_a, η_b, and η_c defined as usual

$$\eta_a = \nu_2 ,$$
$$\eta_b = \nu_3 + \tfrac{1}{4}\gamma_1(1-\lambda)^2 , \tag{B1}$$
$$\eta_c = \nu_3 + \tfrac{1}{4}\gamma_1(1+\lambda)^2 .$$

In addition, we introduce another set of derived viscosity coefficients

$$\alpha_2 = \tfrac{1}{2}(\eta_b - \eta_c - \gamma_1) ,$$
$$\alpha_3 = \tfrac{1}{2}(\eta_b - \eta_c + \gamma_1) ,$$
$$\eta_4 = \tfrac{1}{2}(\eta_b + \eta_c - \gamma_1) , \tag{B2}$$
$$N = 2\nu_1 - 2\eta_4 + \eta_a ,$$

and we define a set of auxiliary quantities in terms of the reduced wave number Q:

$$R_1^2 = 1 + Q_y^2 ,$$
$$R_{1y}^2 = -\alpha_2 Q_x^2 + \alpha_3 Q_y^2 ,$$
$$R_{1z}^2 = -\alpha_2 Q_x^2 + \alpha_3 , \tag{B3}$$
$$R_{2y}^2 = \eta_c Q_x^2 + \left[\eta_a + \eta_b \frac{Q_y^2}{Q_x^2}\right] R_1^2 + N Q_y^2 ,$$
$$R_{2z}^2 = \eta_c Q_x^2 + \left[\eta_a + \eta_b \frac{1}{Q_x^2}\right] R_1^2 + N .$$

The viscosity components then read $\{D = Q_x^2[Q_y^2(N + \eta_b Q_x^{-2} R_1^2)^2 - R_{2y}^2 R_{2z}^2]\}$

$$\gamma_{yy} = 1 + \frac{1}{\gamma_1}\frac{(R_{1y}^2)^2 R_{2z}^2 + \alpha_3^2 Q_y^2[R_{2y}^2 - 2\alpha_3^{-1} R_{1y}^2(N+\eta_b Q_x^{-2} R_1^2)]}{D} ,$$
$$\gamma_{zz} = 1 + \frac{1}{\gamma_1}\frac{(R_{1z}^2)^2 R_{2y}^2 + \alpha_3^2 Q_y^2[R_{2z}^2 - 2\alpha_3^{-1} R_{1z}^2(N+\eta_b Q_x^{-2} R_1^2)]}{D} , \tag{B4}$$
$$\gamma_{yz} = \gamma_{zy}^* = i\frac{1}{\gamma_1}\frac{Q_y[\alpha_3(R_{1y}^2 R_{2z}^2 + R_{2y}^2 R_{1z}^2) - (R_{1z}^2 R_{1y}^2 + \alpha_3^2 Q_y^2)(N+\eta_b Q_x^{-2} R_1^2)]}{D} .$$

The elastic components admit very simple expressions in terms of reduced elastic constants, $\bar{K}_i = K_i / K_1$ $(i=2,3)$ and reduced magnetic fields, $h^2 = H^2 / H_c^2$,

$$\begin{aligned} K_{yy} &= -(\bar{K}_3 Q_x^2 + Q_y^2 + \bar{K}_2) , \\ K_{zz} &= -(\bar{K}_3 Q_x^2 + \bar{K}_2 Q_y^2 + 1 - h^2) , \\ K_{yz} &= K_{zy}^* = -iQ_y(1-\bar{K}_2) . \end{aligned} \tag{B5}$$

Finally, two well-differentiated noise contributions participate in $\bar{\psi}$:

$$\bar{\psi} = \frac{1}{\chi_a H_c^2}(\gamma_1 \underline{\gamma} \bar{\xi} + \bar{\vartheta}) , \tag{B6}$$

the first one, $\bar{\xi}$, directly related to the dynamics of the distortion modes,

$$\bar{\xi} \equiv \begin{bmatrix} \xi_y \\ \xi_z \end{bmatrix} ,$$

and the second contribution $\bar{\vartheta}$ arising from the dynamics of the velocity field modes,

$$\begin{aligned} \vartheta_y = \rho \frac{1}{D} \{ & [\alpha_3 Q_y^2 (N + \eta_b Q_x^{-2} R_1^2) - R_{1y}^2 R_{2z}^2] \zeta_1 \\ & - \alpha_3 Q_y [R_{2y}^2 - \alpha_3^{-1} R_{1y}^2 (N + \eta_b Q_x^{-2} R_1^2)] \zeta_2 \} , \end{aligned} \tag{B7}$$

$$\begin{aligned} \vartheta_z = \rho \frac{i}{D} \{ & [R_{1z}^2 R_{2y}^2 - \alpha_3 Q_y^2 (N + \eta_b Q_x^{-2} R_1^2)] \zeta_2 \\ & + \alpha_3 Q_y [R_{2z}^2 - \alpha_3^{-1} R_{1z}^2 (N + \eta_b Q_x^{-2} R_1^2)] \zeta_1 \} , \end{aligned}$$

where

$$\begin{aligned} \zeta_1 &= Q_x Q_y (\zeta_{xx} - \zeta_{yy}) + (Q_y^2 - Q_x^2) \zeta_{xy} \\ &\quad + i(Q_y \zeta_{xz} - Q_x \zeta_{yz}) , \\ \zeta_2 &= Q_x (\zeta_{xx} - \zeta_{zz}) + i(1 - Q_x^2) \zeta_{xz} \\ &\quad + Q_y (\zeta_{xy} - i Q_x \zeta_{yz}) . \end{aligned}$$

[1] P. G. de Gennes, *The Physics of Liquid Crystals* (Clarendon, Oxford, 1975); S. Chandrasekhar, *Liquid Crystals* (Cambridge University Press, Cambridge, England, 1977); M. J. Stephen and J. P. Straley, Rev. Mod. Phys. **46**, 617 (1974).

[2] E. F. Carr, Mol. Cryst. Liq. Cryst. **34**, L159 (1977).

[3] E. Guyon, R. Meyer, and J. Salán, Mol. Cryst. Liq. Cryst. **54**, 261 (1979).

[4] L. J. Yu and A. Saupe, J. Am. Chem. Soc. **102**, 4879 (1980).

[5] J. Charvolin and Y. Hendrikx, J. Phys. (Paris) Lett. **41**, L597 (1980).

[6] H. Lee and M. M. Labes, Mol. Cryst. Liq. Cryst. **84**, 137 (1982).

[7] F. Lonberg, S. Fraden, A. J. Hurd, and R. B. Meyer, Phys. Rev. Lett. **52**, 1903 (1984).

[8] A. J. Hurd, S. Fraden, F. Lonberg, and R. B. Meyer, J. Phys. (Paris) **46**, 905 (1985).

[9] Y. W. Hui, M. R. Kuzma, M. San Miguel, and M. M. Labes, J. Chem. Phys. **83**, 288 (1985).

[10] M. R. Kuzma, Phys. Rev. Lett. **57**, 349 (1986); D. V. Rose and M. R. Kuzma, Mol. Cryst. Liq. Cryst. Lett. **4**, 39 (1986).

[11] S. Fraden and R. B. Meyer, Phys. Rev. Lett. **57**, 3122 (1986).

[12] M. San Miguel and F. Sagués, Phys. Rev. A **36**, 1883 (1987).

[13] F. Sagués, F. Arias, and M. San Miguel, Phys. Rev. A **37**, 3601 (1988).

[14] F. Sagués, preceding paper, Phys. Rev. A **38**, 5360 (1988).

[15] P. C. Hohenberg and B. I. Halperin, Rev. Mod. Phys. **49**, 435 (1977).

[16] J. D. Gunton, M. San Miguel, and P. S. Sahni in *Phase Transitions and Critical Phenomena,* edited by C. Domb and J. L. Lebowitz (Academic, New York, 1983), Vol. 8.

[17] For general references see Ref. 16; also see P. C. Hohenberg and D. R. Nelson, Phys. Rev. B **20**, 2665 (1979).

[18] F. Sagués and M. San Miguel, Phys. Rev. A **33**, 2769 (1986).

[19] K. Binder, Phys. Rev. A **29**, 341 (1984).

[20] This approximation consists in a sort of linearization of the director contributions to the equations for the velocities whereby $\mathbf{n}$ is replaced by $\mathbf{n}^0$ retaining in this way the initial coupling between $\mathbf{v}$ and $\mathbf{n}$ which is essential at the initial stages of the evolution. For more details see Refs. 12 and 13.

[21] For the nematic phase this free energy consists of the usual Oseen-Frank distortion energy supplemented with the magnetic term and additionally it comprises kinetic and pressure contributions. These last contributions are incorporated to account for the displacements of the nematic molecules. The final explicit expression for $\mathcal{F}$, not explicitly needed in our presentation here, corresponds to Eq. (2.6) of Ref. 12.

[22] In all the calculations we have done it happens that of the pair of eigenvalues, λ_y remains always negative, λ_z being the one truly responsible for the Fréedericksz instability.

[23] According to the definition of τ_0 given in Sec. II and for a typical sample ($d \simeq 10^{-2}$ cm) of MBBA at room temperatures $\tau_0 \simeq 10$ sec.

[24] As a matter of fact, in the pure twist Fréedericksz transition we also found several examples of coexistence of maxima, but in all the cases studied this coexistence was ephemeral and limited to extremely short time intervals corresponding to the very initial phase of the pattern development.

[25] A more in-depth discussion of all these effects is contained in the original paper by Hurd *et al.* (Ref. 8).